JOURNAL OF MATERIALS SCIENCE 30 (1995) 3005–3009

Reactivity of perovskites on oxidative coupling of methane

M. TEYMOURI, E. BAGHERZADEH
NIOC Research Institute, P.O. Box 1863, Taleghan Avenue, Tehran, Iran
C. PETIT, J. L. REHSPRINGER, S. LIBS, A. KIENNEMANN
LERCSI URA 1498, EHICS 1, rue Blaise Pascal 67000 Strasbourg, France

Well-defined structures like ABO_3 (A = Ba, Sr, Ca; and B = Ti, Zr) perovskites were prepared by a sol–gel method which permits the formation of a crystalline structure at low-calcination temperatures (~700 °C). The perovskite structures were characterized by X-ray diffraction (XRD), scanning electron microscopy (SEM) and Brunauer–Emmett–Teller (BET) methods and the carbonate present at the surface was determined by Fourier transform infra-red spectroscopy. Reactivity studies showed that the perovskite structures are stable under oxidative coupling of methane (OCM) conditions. The yield increases followed the sequence Ca < Sr < Ba and Zr < Ti, and a stable $BaTiO_3$ gives a C_2 yield of 15% at 800 °C.

1. Introduction

In the last fifteen years, there has been much research on chemicals and liquid transportation fuel production from non-petroleum-fossil carbon sources. An extensive part of this research is now devoted to the utilization of natural gas as a source for chemicals and fuels [1, 2]. Indeed, natural gas is largely considered to be an under-utilized carbon-containing feedstock. Its conversion to chemicals and fuels can be beneficial for both economic and environmental reasons. There are two main methods: indirect transformation (through syngas and its reactions) or direct conversion to chemicals (methanol and mainly hydrocarbons). An examination of the economics of these different processes shows that the major cost of the indirect transformations is related to the syngas production. Therefore, direct conversion of methane seems to be an economically reasonable pathway to its valorization. However, the high stability of methane and the unfavourable thermodynamics clearly indicate the difficulties which must be overcome in direct methane activation [1]. Since the direct dehydrogenation of methane to ethylene or ethane is thermodynamically prohibited ($\Delta G > 0$), the use of a hydrogen acceptor co-substrate (O_2, N_2O, halogen or unsaturated hydrocarbons) is required to make the overall transformation thermodynamics favourable. With oxygen, two types of valuable products can be obtained: methanol and C_2 hydrocarbons. A small part of the recent work has focused on direct methanol formation [3], but to a large extent the search for an efficient catalytic material has been unsuccessful.

The major part of the effort has been directed to the oxidative coupling of methane (OCM) [4–6]. At present, a C_2 hydrocarbon yield of 25% seems to be the upper limit which can be achieved. This limit is too low to allow industrial development [7].

Numerous compounds have been tested as catalysts in OCM and a definitive classification of these catalysts would be very difficult. However, one can roughly distinguish three groups containing alkali and alkaline earths, lanthanides or transition and post-transition metals [6]. Among the alkali- and alkaline-earth oxides, Li_2O, Na_2O, CaO, BaO or SrO are used as precursors or dopants. It is noteworthy that in Li/MgO, Na/CaO or Sr/La_2O_3 systems the alkali or alkaline earth cannot strictly be considered as being deposited on the support, and, since the radii of both cations are close to each other, exchange of the two cations can occur on the catalytic surface [8, 9]. Therefore, well-defined structural compounds (like $LnLiO_2$ (Ln = rare earth) [10, 11], pyrochlores [12, 13] and perovskites [14, 15]) containing the above-mentioned elements were considered to be of interest in the OCM. The ABO_3 perovskite structure fits particularly well in forming numerous combinations of elements with different valencies $A^{n+}B^{m+}$ ($n = 1, 2, 3$; $m = 5, 4, 3$) or to allow the substitution of cations leading to a mixed structure, $AA'BB'O_3$ [16]. These combinations can lower the element–oxygen bond strength and favour breaking of these bonds resulting in surface vacancies, O^- or O^{2-} species, which are potential intermediates in oxidative coupling [17, 18]. Thus, many well-defined structures have been proposed for total oxidation of methane to CO_2–$LaCrO_3$ [19], $LaCoO_3$ [20, 21] – or for the oxidative coupling–three metallic [22, 23], lithium [24] or alkaline-earth doped systems [25]. The aim of the present work was to test the OCM activity of ABO_3 perovskite compounds (A = Ba, Sr, Ca; and B = Ti, Zr) prepared by sol–gel methods.

0022–2461

2. Experimental procedure

2.1. Catalyst preparation

ABO_3 perovskites (A = Ba, Sr, Ca; and B = Ti, Zr) were prepared by a sol–gel process. The alkaline-earth oxides or acetate were dissolved in an excess of propionic or butyric (for Ca) acid.

The amount of Ti or Zr required to form the perovskite structure was added as a propionic acid solution of Ti or Zr isopropionate. A transluscent solid was obtained by solvent evaporation. This solid was then calcined between 650 and 1000 °C to form the desired well-defined structure. The standard annealing condition of the samples was 750 °C for 4 h, with the rate of heating being 3 °C min^{-1}.

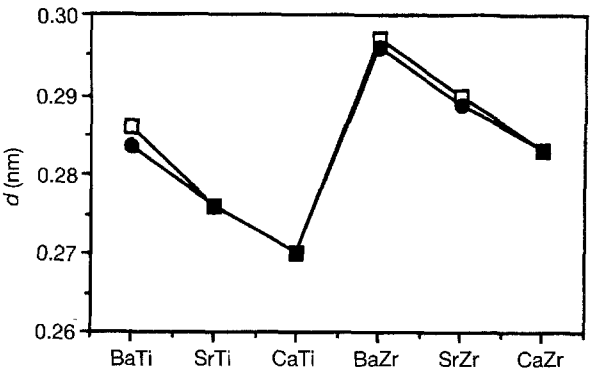

Figure 1 The most intense XRD peak for ABO_3 catalysts: (□) prepared in the laboratory (T_{cal} = 750 °C); (●) the published data.

2.2. Apparatus and conditions for catalytic tests

The activity and selectivity of the various samples were determined in a fixed-bed quartz reactor (6.6 mm) internal diameter under the following conditions: temperature area, 400–800 °C; gas flow, 7.5 to 30 $l h^{-1} g^{-1}$ (at (STP)); a CH_4/O_2 ratio of between 2 and 20; feed-gas partial pressures given for $CH_4/O_2 = 2$ of 0.133 atm CH_4, 0.0665 atm O_2 and 0.8 atm He. The CH_4, O_2 and He flows were controlled by an electronic-mass-flow metering system. The gases were mixed before introduction into the quartz reactor. The temperature was measured by a thermocouple placed near the catalytic bed. The reactant and products were analysed by gas chromatography (TCD) on Carbosphere and Porapak Q column packings. The main reaction products were CO, CO_2, C_2H_4, C_2H_6 and H_2O. C_3 and C_4 hydrocarbons were produced in trace amounts and they were not measured systematically.

3. Results and discussion

3.1. Characterization of the perovskites

X-ray diffraction (XRD) data for ABO_3 solids (A = Ba, Sr; and B = Ti, Zr) calcined at 700 °C and at 750 °C (A = Ca) show that the perovskite structure is readily formed by our preparation method. The positions of the most intense line of the perovskites given in the literature and obtained experimentally after calcining at 700 or 750 °C are represented on Fig. 1. The good fitting of the experimental and the reference data [26–28] indicate the successful preparation of these structures. Except for $SrTiO_3$, this preparation only leads to the formation of perovskites, no other species (oxide, carbonate, well-defined structure) was obtained by XRD. For $SrTiO_3$, compounds with a neighbouring stoichiometry ($Sr_2Ti_2O_7$, $Sr_4Ti_3O_{10}$) can be formed, and this makes the choice of the annealing conditions very important (calcination at 650 °C under a CO_2-free air flow). Increasing the annealing temperature from 700 to 1000 °C for $BaTiO_3$, $BaZrO_3$ and $SrTiO_3$ results in a more well-structured product (more intense and finer lines) but the same characteristics remain (number and position of lines, intensity ratios). Fig. 2 shows XRD spectra of $BaTiO_3$ for two calcination temperatures (700 and 1000 °C), before and after running in OCM. The perovskite structure of $BaTiO_3$ is retained after the catalytic test. All the perovskites tested had good stabilities.

The Brunauer–Emmett–Teller (BET) specific areas of the perovskites were measured for different component elements and calcination temperatures (between 650 and 1000 °C). There is an ideal temperature for the formation of the desired structure, depending on the elements introduced. At lower temperatures, the specific BET surface area is high. It diminishes by further heating to this ideal temperature. The standard calcination at 750 °C is sufficient to obtain stable structures for all the perovskites studied. The surface areas obtained (between 3 and 10 $m^2 g cat^{-1}$) show this dependence on the starting elements. Carbonate species (for Ba, Sr and Ca) formed during the calcination were detected by Fourier-transform infrared (FTIR) spectroscopy. The amount of carbonates formed is always low, and remains unchanged during the catalytic test.

The results of scanning electron microscopy (SEM) of $BaTiO_3$ calcined at 700 and 1000 °C are shown in Fig. 4 before and after catalytic testing. The surface of the catalyst was uniform and consisted of little beads sticking to each other. For $BaTiO_3$, more porous beads stuck to each other. For $BaTiO_3$ more porous beads were observed for the sample calcined at 700 °C than for that annealed at 1000 °C. After the reaction, the beads had a molten aspect, and this explains the reduction of the surface area during the catalytic test for the sample calcined at 700 °C.

3.2. Catalytic reactivity measurements

3.2.1. Ageing

The stabilities of the perovskite structures observed by the different characterization means (XRD, BET, FTIR and SEM) were confirmed by the catalyst ageing studies under the OCM conditions. The ageing of $BaTiO_3$ calcined at 750 °C is given in Fig. 5. No changes in the oxygen and methane conversion or the product distribution formed were observed. This was valid for all the perovskite structures studied.

3.2.2. Catalytic activity

The catalytic behaviour versus the reaction temperature is given in Fig. 6 for $BaTiO_3$ calcined at 750 °C.

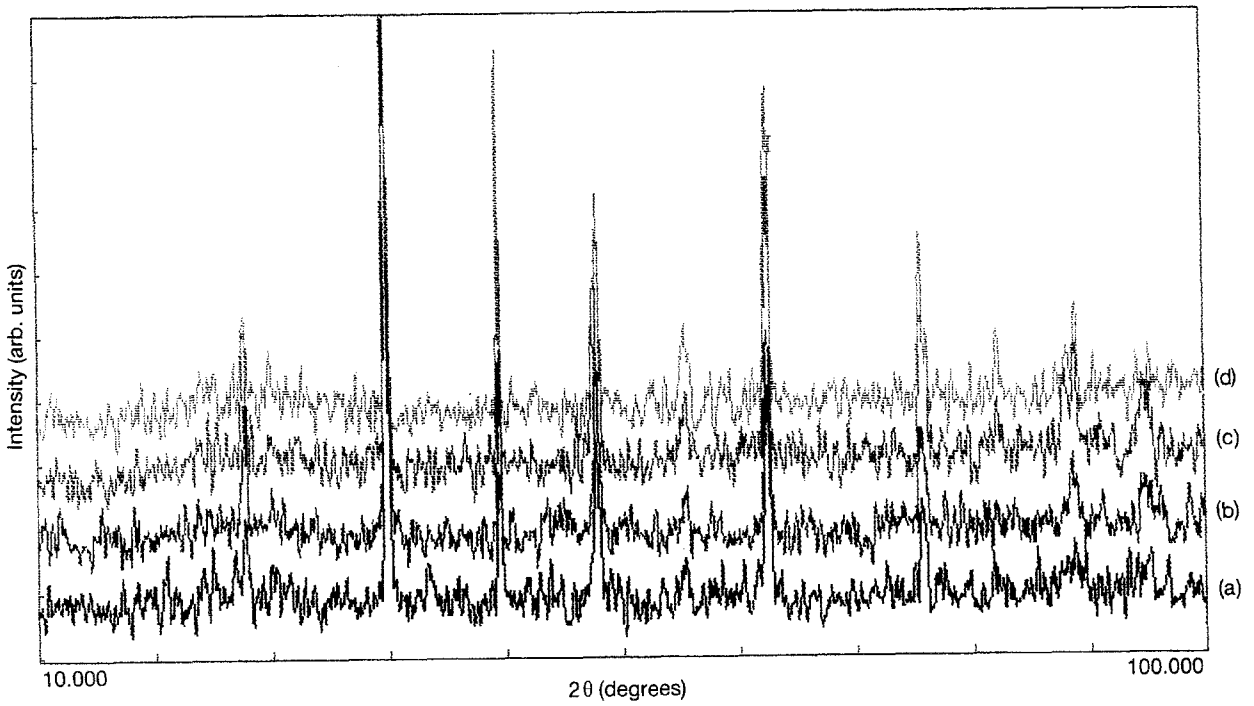

Figure 2 XRD data (using Co$K_{\alpha 1}$ radiation) for $BaTiO_3$ calcined: at 700 °C (a) before and (b) after testing; and at 1000 °C (c) before and (d) after testing.

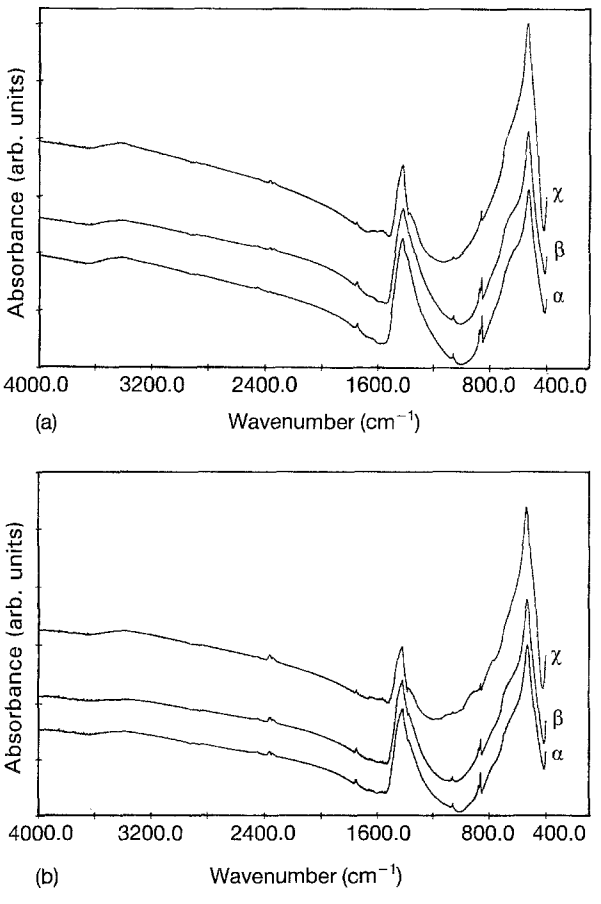

Figure 3 (a) FTIR spectra for $BaZrO_3$ as a function of the calcination temperature: (a) before testing (α) at 700 °C, (β) at 750 °C and (χ) at 1000 °C; and (b) after testing (α) at 700 °C, (β) at 750 °C and (χ) at 1000 °C.

The behaviour is almost the same for all the perovskites studied except for $CaZrO_3$. An area with high oxidating characteristics is observed between 450 and 635 °C (part 1) and only CO and CO_2 are formed. In this area, the methane and oxygen conversions increase quickly as the temperature is enhanced. The oxidative reaction begins at higher temperatures for those catalysts which are active in OCM except for $CaZrO_3$. The CO selectivity decreases as the temperature increases. As shown in Fig. 7 for $CaZrO_3$, the CO selectivity is more than 50% at 500 °C, whereas it reaches only 10% for $BaTiO_3$ and $SrTiO_3$. In part 2 of Fig. 6, the oxygen conversion is near to 100% and that of methane further increases but more slowly from 25% and upward, this is related to an enhanced C_2 selectivity (a CH_4/O_2 ratio of 2). Ethane is never obtained at temperatures lower than 630 °C. Ethylene appears even at higher temperatures. Table I shows that the temperature at which C_2 appears depends strongly on the nature of the catalyst. Moreover, the lower the minimal C_2-appearance temperature is, the higher is the maximum C_2 yield.

For all catalysts studied, the presence of Ti is more favourable than that of Zr in the perovskite structure. The C_2 hydrocarbon selectivity, and the methane and oxygen conversions, are higher in the presence of Ti. Furthermore an increase in the CH_4/O_2 ratio from 2 to 5 leads to an 80% C_2 selectivity for $BaTiO_3$, whereas only 40% can be reached for $BaZrO_3$. The results obtained with $CaTiO_3$ and $CaZrO_3$ confirm that Ti perovskites are better than those of Zr in OCM. For Ti and Zr perovskites, the conversion and the C_2 selectivity increase in the following sequence:

$$Ca < Sr < Ba$$

This reactivity sequence can be partly explained by taking into consideration the perovskite structure. The ideal perovskite structure is cubic and the coordination number is 12 and 6 oxygen atoms, respectively, for A and B. An increase in the ionic radii for

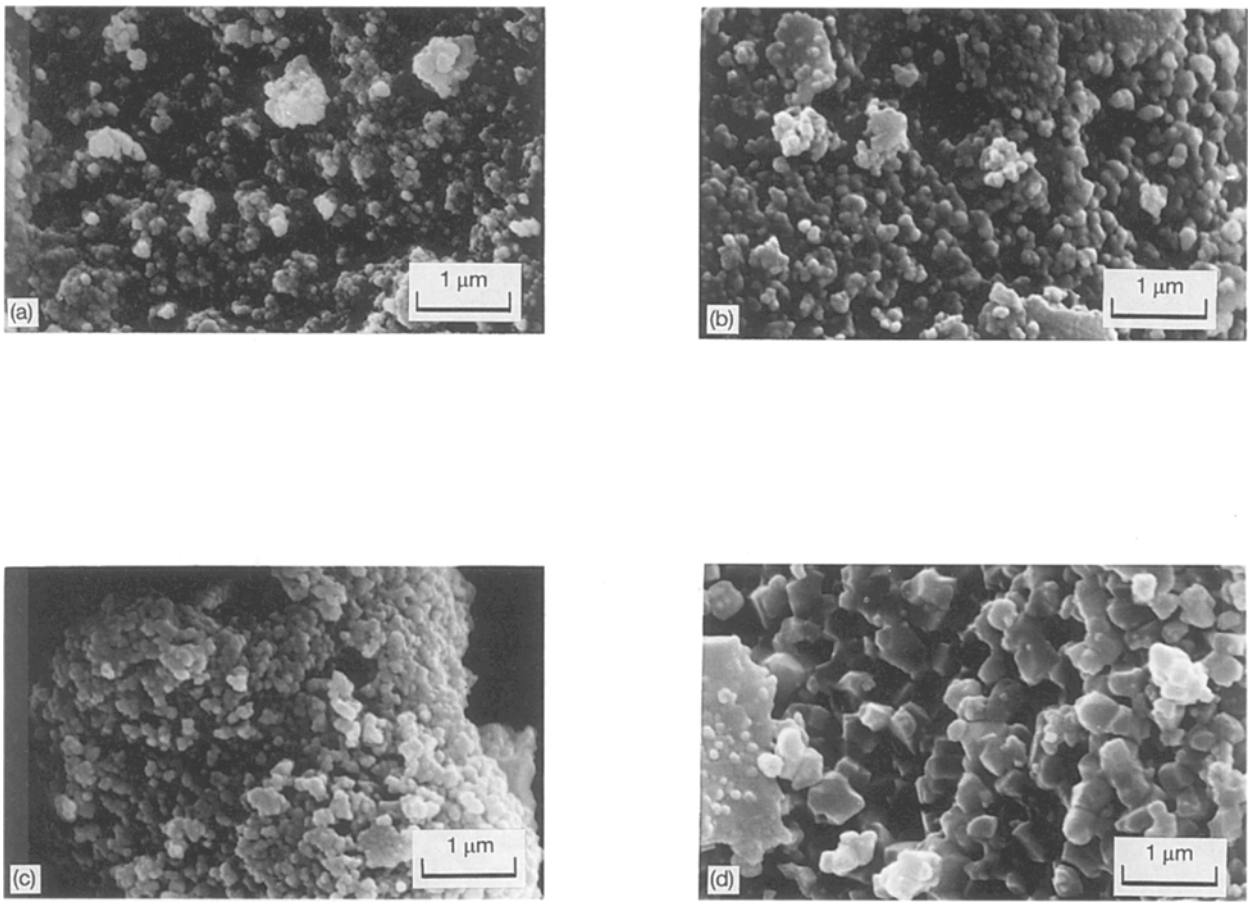

Figure 4 MEB of $BaTiO_3$ calcined at 700 °C (a) before and (b) after testing; and calcined at 1000 °C (c) before and (d) after testing.

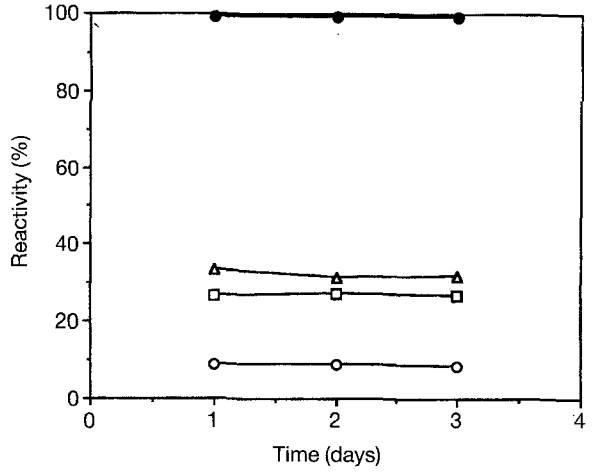

Figure 5 Reactivity of $BaTiO_3$ calcined at 750 °C versus time. (-□-) conversion of CH_4, (-●-) conversion of O_2, (-△-) selectivity into C_2 and (-○-) yield into C_2.

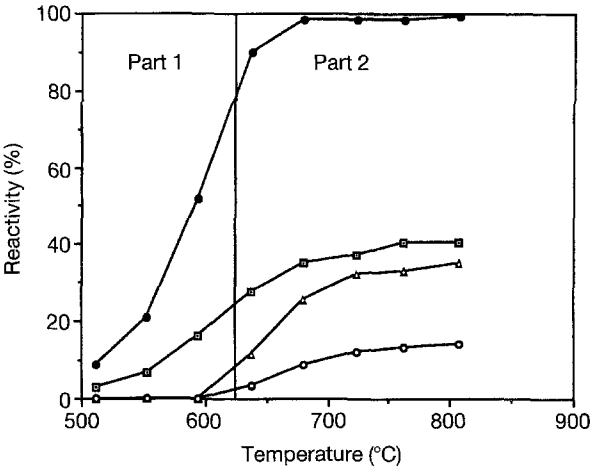

Figure 6 Results of $BaTiO_3$ calcined at 750 °C versus the temperature of reaction for a ratio of CH_4/O_2 equal to 2. (-⊡-) conversion of CH_4, (-●-) conversion of O_2, (-▲-) selectivity into C_2 and (-○-) yield into C_2.

$Ba^{2+} < Sr^{2+} < Ca^{2+}$ at a co-ordination number of 12 leads to an increase in the lattice parameters; this is related to a position shift of the most intensive line of the XRD spectra for the Ti and Zr perovskites (Fig. 1). The Ti^{4+} ionic radius (0.1944 nm) is lower than that of Zr^{4+} (0.2174 nm) at a co-ordination number of 6, and this results in a smaller lattice parameter. For all catalytic systems, the C_2 selectivity is significantly enhanced when the oxygen conversion is total. This experimental feature suggests that the oxidation reaction is performed by two different types of oxygen which are present on the catalytic surface: adsorbed oxygen and lattice oxygen. Indeed, it has been shown [20, 29] that perovskites can adsorb and desorb important amounts of oxygen, and that their lattice oxygen could be active. The adsorbed oxygen is less strongly held by the surface and can, therefore, react at lower temperatures and lead to total CH_4 combustion. On $BaTiO_3$ and $BaZrO_3$ for example, Vermeiren *et al.* [22] have observed, by adsorption of methane

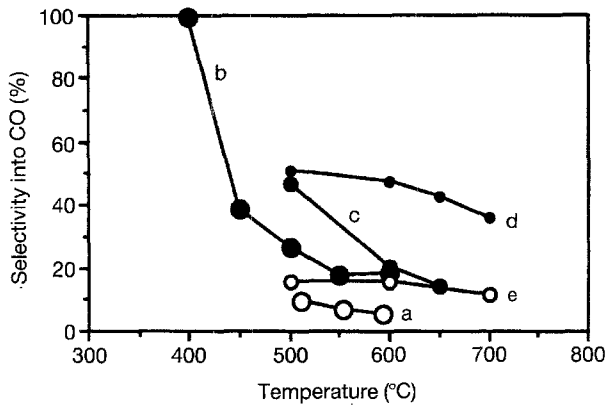

Figure 7 Selectivity into CO of perovskites at low reaction temperatures (400–700 °C): (a) $BaTiO_3$, (b) $BaZrO_3$, (c) $SrZrO_3$, (d) $CaZrO_3$, and (e) $SrTiO_3$.

TABLE I The relation between the minimal C_2-formation temperature and the maximum C_2 yield that can be achieved

Catalysts	Minimal C_2 formation temperature, T (°C)	Maximum C_2 yield (%)
$BaTiO_3$	637	15
$BaZrO_3$	650	9
$SrTiO_3$	650	8.5
$SrZrO_3$	700	6
$CaTiO_3$	720	3

after $^{18}O_2$ adsorption, that the CO_2 formed at low temperatures contains only oxygen from the gas phase without participation by the lattice oxygen of the perovskite structure. It is only when the oxygen conversion is almost total, as the temperature is increased, that the lattice oxygen sites of the perovskite structure become accessible and/or active in the mild oxidation. This participation by the lattice oxygen results in the formation of surface oxygen vacancies, as has already been observed on $BaTiO_3$ and $BaZrO_3$ [22]. Once these vacancies are formed, the switch to C_2 hydrocarbons could be represented by the scheme proposed by Ekstrom and Lapszewick [30].

4. Conclusion

This work shows that on ABO_3 perovskites (A = Ba, Sr, Ca; B = Ti, Zr) the yields of C_2 hydrocarbons decrease from Ti to Zr, and from Ba to Ca. C_2 hydrocarbons are only observed when the oxygen conversion is almost complete, and a relation exists between the minimal temperature where C_2 products are formed and the maximum C_2 yield. Therefore, it is suggested that CO_2 and C_2 hydrocarbons are obtained by reaction of adsorbed or lattice oxygen, respectively.

References

1. M. S. SCURELL, *Appl. Catal.* **32** (1987) 1.
2. H. MIMOUN, *New. J. Chem.* **11** (1987) 1.
3. N. R. FORSTER, *Appl. Catal.* **19** (1985) 1.
4. R. BURCH, G. D. SQUIRE and S. C. TSANG, *ibid.* **43** (1988) 105.
5. G. J. HUTCHINGS, M. S. SCURELL and J. R. WOODHOUSE, *Chem. Soc. Rev.* **18** (1989) 251.
6. Y. AMENOMIYA, V. I. BIRSS, M. GOLUDZINOWSKI, J. GALUSKA and A. R. SANGER, *Catal. Rev. Sci. Engng.* **32** (1990) 163.
7. J. A. LABINGER, *Catal. Lett.* **1** (1988) 371.
8. K. I. AIKA and T. NIGHIYANA, *Stud. Surf. Sci. Catal.* **61** (1991) 165.
9. C. H. LIU, T. ITO, J. X. WANG and J. H. LUNSFORD, *J. Amer. Chem. Soc.* **109** (1987) 4808.
10. J. L. REHSPRINGER, A. KADDOURI, P. POIX and A. KIENNEMANN, *Stud. Surf. Sci. Catal.* **63** (1991) 575.
11. A. KIENNEMANN, R. KIEFFER, A. KADDOURI, P. POIX and J. L. REHSPRINGER, *ibid.* **55** (1990) 365.
12. C. PETIT, J. L. REHSPRINGER, A. KADDOURI, P. POIX and A. KIENNEMANN, *Catal. Today* **13** (1992) 409.
13. C. PETIT, A. KADDOURI, S. LIBS, A. KIENNEMANN, J. L. REHSPRINGER and P. POIX, *J. Catal* **140** (1993) 328.
14. H. NAGAMOTO, K. AMANUMA, H. NOBUTOMO and H. INOUE, *Chem. Lett.* (1988) 237.
15. Y. CHUNYING, L. WENZHAO, F. WENJA, Q. AIHUA and C. YIXIAN, Chem. Proceedings of the 10th International Congress on Catalysis, paper 075, 19–24 July 1992, Budapest.
16. L. G. TEJUCA, J. L. G. FIERRO and J. TASCON, *Adv. Catal.* **36** (1989) 237.
17. E. R. S. WINTER, *J. Chem. Soc. A.* (1988) 2889.
18. T. ITO, J. X. WONG, C. H. LIN and J. H. LUNSFORD, *J. Amer. Chem. Soc.* **107** (1985) 5062.
19. B. DE COLLONGUE, E. GARBOWSKI and M. PRIMET, *J. Chem. Soc. Faraday Trans.* **87** (1991) 2493.
20. T. SEIYAMA, N. YAMAZOE and K. EGUCHI, *Ind. Engng. Chem. Prod. Res. Dev.* **24** (1985) 19.
21. Z. KAIJI, L. JIAN and B. YINGLI, *Catal. Lett.* **1** (1988) 299.
22. W. J. M. VERMEIREN, I. D. M. L. LENOTTE, J. A. MARTENS and P. A. JACOBS, *Stud. Surf. Sci. Catal.* **61** (1991) 33.
23. Z. KAIJI, L. YU, B. YINGLI and W. QUAN, *ibid.* **61** (1991) 123.
24. Z. KALENIK and E. E. WOLF, *ibid.* **61** (1991) 97.
25. K. AIKA and T. NISHIYAMA, *ibid.* **61** (1991) 165.
26. National Bureau of Standards (US), Monograph 25 (1971).
27. M. AHTEE *et al.*, *Acta Cryst.* B **34** (1978) 752.
28. SWANSON *et al.*, National Bureau of Standards (US), Circular 539, (1955) p. 58.
29. H. ARAI, T. YANADA, K. EGUCHI and T. SELYAMA, *Appl. Catal.* **26** (1986) 265.
30. A. EKSTROM and J. A. LAPSZEWICZ, *J. Phys. Chem.* **93** (1989) 5230.

Received 5 February
and accepted 18 August 1993